Theory of relaxation dynamics in glass-forming hydrogen-bonded liquids

H. G. E. Hentschel[1,2] and Itamar Procaccia[1]
[1]*Department of Chemical Physics, The Weizmann Institute of Science, Rehovot 76100, Israel*
[2]*Department of Physics, Emory University, Atlanta, Georgia 30322, USA*
(Received 7 September 2007; revised manuscript received 4 October 2007; published 27 March 2008)

We address the relaxation dynamics in hydrogen-bonded supercooled liquids near (but above) the glass transition, measured via broadband dielectric spectroscopy (BDS). We propose a theory based on decomposing the relaxation of the macroscopic dipole moment into contributions from hydrogen-bonded clusters of s molecules, with $s_{\min} \leq s \leq s_{\max}$. The existence of $s_{\max}$ is translated into a sum rule on the concentrations of clusters of size s. We construct the statistical mechanics of the supercooled liquid subject to this sum rule as a constraint, to estimate the temperature-dependent density of clusters of size s. With a theoretical estimate of the relaxation time of each cluster, we provide predictions for the real and imaginary parts of the frequency-dependent dielectric response. The predicted spectra and their temperature dependence are in accord with measurements, explaining a host of phenomenological fits like the Vogel-Fulcher fit and the stretched exponential fit. Using glycerol as a particular example, we demonstrate quantitative correspondence between theory and experiments. The theory also demonstrates that the α peak and the "excess wing" stem from the same physics in this material. The theory also shows that in other hydrogen-bonded glass formers the excess wing can develop into a β peak, depending on the molecular material parameters (predominantly the surface energy of the clusters). We thus argue that α and β peaks can stem from the same physics. We address the BDS in constrained geometries (pores) and explain why recent experiments on glycerol did not show a deviation from bulk spectra. Finally, we discuss the dc part of the BDS spectrum and argue why it scales with the frequency of the α peak, providing an explanation for the remarkable data collapse observed in experiments.

DOI: 10.1103/PhysRevE.77.031507 PACS number(s): 64.70.P−, 77.22.Gm

I. INTRODUCTION

In this paper we propose a theory, based on a simple physical model at the mesoscale, that can account quantitatively for most of the observed features in the remarkable relaxation dynamics of glass-forming hydrogen-bonded liquids [1–8]. The paradigmatic example of such systems is dry glycerol and glycerol-water mixtures, but other alcohols and alcohol mixtures show similar properties. The relaxation dynamics of such systems in the vicinity of the glass transition exhibit an extremely wide range of frequencies, spanning sometimes 16 orders of magnitude or more in the frequency domain. Despite the fact that good measurements have been available for more than half a century [1], and after considerable experimental and theoretical effort, including apparent "first-principles" theories like mode coupling [9], there is no accepted derivation of the observed characteristics of the relaxation dynamics. Until now most discussions of experimental data are limited to fitting phenomenological expressions that are not the result of a proper theory [10]. The present paper attempts to close this gap.

An excellent technique to probe this enormous range of frequencies is broadband dielectric spectroscopy (BDS) which covers the frequency band (10^{-5}–10^{11} Hz) and temperature range (100–600 K). The interpretation of the measurements in BDS is facilitated by the fact that the dielectric theory for BDS is well established and independent of the nature of the relaxational mechanisms involved in any particular material and at any particular temperature and pressure. We can express the frequency-dependent dielectric constant $\epsilon(\omega)$ in terms of the Laplace-Fourier transform

$$\frac{\epsilon(\omega)-\epsilon_\infty}{\epsilon_0-\epsilon_\infty} = \int_0^\infty \left(\frac{-d\phi(t)}{dt}\right) e^{-i\omega t} + \frac{4\pi i \sigma_{\rm dc}/(\epsilon_0-\epsilon_\infty)}{\omega}. \quad (1)$$

Here ϵ_∞ is the high-frequency dielectric constant due to fast rotational processes above 10^{12} Hz and atomic polarization; ϵ_0 is the static dielectric constant; and $\sigma_{\rm dc}$ is the dc conductivity of the medium. The response function $\phi(t)$ is given by the normalized correlation function of the macroscopic dipole moment $\mathbf{M}(t)$,

$$\phi(t) = \frac{\langle \mathbf{M}(t)\cdot\mathbf{M}(0)\rangle}{\langle \mathbf{M}(0)\cdot\mathbf{M}(0)\rangle}. \quad (2)$$

A typical BDS absorption spectrum read from the imaginary part of $\epsilon(\omega)$ with dry glycerol at temperature $T=196$ K is shown in Fig. 1. One observes what has been termed in the literature "the main relaxation process" or α peak at $f_{\max} \approx 10^{-1}$ Hz, and then tapering off initially with a typical power law form $\omega^{-\beta}$, which will appear as a straight line on a log-log plot, but is generally followed by a typical wing, which in Fig. 1 has a gentle curvature at frequencies above $f \geq 10^2$ Hz. This part of the spectrum had been termed in the literature "the excess wing." This term does not reflect a deep realization of the existence of an excess loss, but rather the name stems simply from the inability of the phenomenological Davidson-Cole fit formula [11] to agree with the experimental spectrum at this frequency range. While not in glycerol, in other hydrogen-bonded glass formers this wing can also exhibit a clear shoulder or even a distinct second β peak [6]. The literature does not agree on whether the α relaxation and the excess wing (or the β peak when it exists) stem from the same physics or not [7]. A very strong experi-

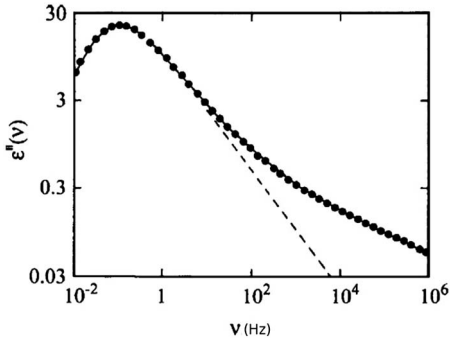

FIG. 1. A typical BDS absorption spectrum read from the imaginary part of $\epsilon(\omega)$ for dry glycerol at temperature $T=196$. The dashed line is the phenomenological Davidson-Cole formula, which fails to describe the so-called excess wing.

mental argument in favor of the very same physics was presented in [8] where spectra taken at different temperatures were rescaled by the position and amplitude of the α peak (see Fig. 2). The excellent data collapse is a strong indication that the α process, the excess wing, and the dc conductivity contribution somehow stem from the same physical mechanism. The theory presented below will corroborate this finding and will clarify the physical origins of the α and β peaks when both exist.

Of course, the raw spectra exhibit a strong temperature dependence. Using spectra measured in the range of temperatures 190–240 K in dry glycerol, the positions of the maxima of the main process have been fitted to the Vogel-Fulcher formula by defining $\tau_{\max}=1/2\pi f_{\max}$ and then writing

$$\tau_{\max}(T) = \tau_v \exp[DT_v/(T-T_v)]. \tag{3}$$

The three parameters were fitted to the data with the results $\ln \tau_v=-35.9$, $D=22.7$, and $T_v=125$ K. Note that this fit implies an attempt time $\tau_v \approx 10^{-16}$ s, which is a very short time indeed. We will argue below that the Vogel-Fulcher formula has no deep meaning, and the parameters involved are of limited physical interest. Although the spectra derived from our theory below will be shown to agree with Eq. (3) in the range of measurement used, we argue that the formula is nothing but a data fit that can be used only in a finite range of temperatures. The prediction of the theory described below is that there is no true divergence of $\tau_{\max}$ at any temperature $T>0$.

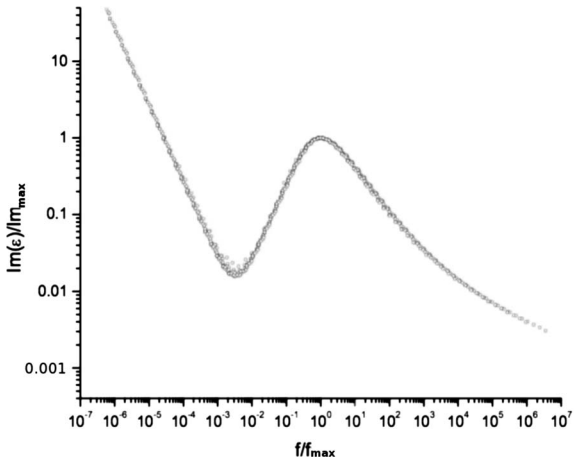

FIG. 2. Experimental BDS absorption spectra of dry glycerol in a range of temperatures 202–292 K, where frequencies were rescaled to the maximum of the α peak and amplitudes were rescaled to the amplitude of the same peak. Note that in comparison to Fig. 1 here the dc contribution is also shown. The data collapse indicates strongly that the α peak, the excess wing, and the low-frequency conductivity contribution all stem from the same physics.

The task of the theorist is then to derive, on the basis of a clearly defined model, the form of the frequency-dependent dielectric response $\epsilon(\omega)$ for this system, to explain the observed spectra (both real and imaginary parts). In particular, a theory should indicate whether the main process and the excess wing stem from the same physics or whether one needs to invoke more than one relaxation mechanism. We will see that the former is the case here. Then one needs to explain the observed fits to the Vogel-Fulcher formula. While the present authors do not ascribe much physical significance to the parameters appearing in the formula, nevertheless the experimental fits should be accounted for, and hopefully the origin of the parameters identified. Finally one needs to explain the remarkable data collapse shown in Fig. 2. We believe that the present paper achieves these tasks.

In order to understand the broadband dielectric spectroscopy of glycerol (and in the future water-glycerol mixtures and other alcohols), we will treat glycerol in the relevant range of temperatures as a heterogeneous fluid on macroscopic time scales. This picture stems from direct experimental observations, for example of the rotational diffusion of dye molecules in supercooled glycerol (cf. [12] and references therein). That is, while on very long time scales the liquid phase must be homogeneous, there exist localized mesoscale domains in the fluid that have macroscopic lifetimes. Indeed, inhomogeneities that appear to survive for 10^4 s contribute to the dielectric response in the Fourier domain at frequencies as low as 10^{-4} Hz in some cases. We shall develop the theory on the basis that these inhomogeneities are a distribution of clusters having the structure of an incipient strongly hydrogen-bonded "frozen" phase and a surrounding bath of more mobile and less dense "liquidlike" glycerol phase. In [17] it was presumed that the molecules in the interiors of the clusters are frozen into energetically favorable glassy configurations, just as in the glassy state below the glass transition. The boundaries between these clusters must then consist of more disordered material. Building on this picture, our task is twofold: first, to express the dielectric response in terms of this cluster distribution; and second, to find the distribution of clusters. We shall do this using mesoscale thermodynamic arguments. Once we have these distributions we describe the resulting BDS, and we shall see the appearance of both a dominant α peak at low frequencies and, depending on molecular parameters, an excess wing or a secondary β shoulder at higher frequencies. We should note that in spirit our approach combines ideas based on the molecular dynamics observations by Geiger and Stanley [13] on the appearance of low-density patches in hydrogen-bonded water (though in the present context we are actually considering higher-density patches in hydrogen-bonded glycerol),

together with ideas of Chamberlin [14] and Kivelson *et al.* [15,16] on treating such heterogeneities as clusters. The similarity to all these theories extends, however, only up to Eq. (6) below, after which our theory diverges from theirs. The crucial differences from previous theories will be pointed out below as we go along. We trust that the reader will find the present approach superior in simplicity and in the quality of the predictions.

In Sec. II we present the dielectric theory for a medium in which there exist clusters whose dipole moments are responsible for the dielectric response. We estimate the rotational relaxation time of such clusters, and, most crucially, their concentrations. In computing the concentrations we deviate most strongly from all previous theories. In Sec. III we specialize the theory to the case of glycerol; it is interesting to see how, by using a modest input of experimental data, we get naturally a host of results in very good correspondence with experiments. We explain the apparent Vogel-Fulcher and stretched exponential fits, but also point out that the range of validity of these fits is finite, whereas the present theory is more widely applicable. Section IV opens up the discussion for other materials, and examines the changes expected in the spectra when molecular parameters change. We show how the relative prominence of the α and β peaks depends on such parameters. In Sec. V we discuss BDS in constrained geometries and explain why glycerol in small pores exhibits the same spectra as bulk glycerol; the explanation is that the smallest pores were just big enough to contain the largest clusters predicted by the theory. Reducing the pores a bit further should result in a dramatic change in the spectra. In Sec. VI we explain how the present model rationalizes the data collapse of the dc conductivity, and in Sec. VII we present a summary and a discussion.

II. DIELECTRIC THEORY FOR CLUSTERS

A. The physical model and the fundamental assumption

We propose that the long-time relaxation in glycerol arises due to the existence of clusters of s molecules which are hydrogen bonded to make the cluster a recognizable entity. We denote the number of clusters of s molecules as N_s. In terms of these clusters, we can write the dipole moment of the system, $\mathbf{M}(t)$, as the sum $\mathbf{M}(t)=\Sigma_\alpha \mathbf{m}_\alpha(t)+\mathbf{M}_{\text{liquid}}(t)$ where $\mathbf{m}_\alpha(t)$ is the dipole moment of cluster α. We expect the rotational relaxations of molecules in the liquid to be fast, and accordingly the fast-relaxing fluid contribution to the dipole moment, $\mathbf{M}_{\text{liquid}}(t)$, will not be studied in detail, as its spectrum is expected to be significant only at high frequencies. We expect that in the supercooled liquid relaxation phenomena are relatively rare events, allowing us to assume that different relaxation events are statistically uncorrelated. This is the fundamental assumption of the model, i.e., that the relaxation process in each cluster is statistically independent of the other clusters. In fact, by a "cluster" we mean a bunch of molecules that are highly correlated; if there are two adjacent clusters that are highly correlated, they should be considered as one cluster. With this in mind we can then write

$$\phi(t) = \frac{\sum_\alpha \langle \mathbf{m}_\alpha(t) \cdot \mathbf{m}_\alpha(0)\rangle}{\sum_\alpha \langle \mathbf{m}_\alpha(0) \cdot \mathbf{m}_\alpha(0)\rangle}. \tag{4}$$

We can rewrite Eq. (4) in terms of an intensive number density $n_s=N_s/M$, where M is the total number of molecules in the system:

$$\phi(t) = \frac{\sum_s n_s\langle \mathbf{m}_s(t) \cdot \mathbf{m}_s(0)\rangle}{\sum_s n_s\langle \mathbf{m}_s(0) \cdot \mathbf{m}_s(0)\rangle}. \tag{5}$$

With each cluster we associate its typical rotational relaxation time τ_s, which only in Sec. VI do we identify with the cluster lifetime. Thus $\phi(t)$ assumes the form

$$\phi(t) = \frac{\sum_s n_s\langle \mathbf{m}_s \cdot \mathbf{m}_s\rangle \exp(-t/\tau_s)}{\sum_s n_s\langle \mathbf{m}_s \cdot \mathbf{m}_s\rangle}. \tag{6}$$

To proceed further we need to estimate n_s, $\langle \mathbf{m}_s \cdot \mathbf{m}_s\rangle$, and τ_s. We start with the static dipole correlations.

B. The static dipole correlations

The dipole moment of a cluster of size s can be expressed in terms of individual glycerol molecule dipoles $\mathbf{d}_i$ as $\mathbf{m}_s=\Sigma_{i=1}^s \mathbf{d}_i$. For a set of noninteracting dipoles $\langle \mathbf{m}_s \cdot \mathbf{m}_s\rangle = sd^2$, where $d=|\mathbf{d}_i|$. We do not expect the dipoles in the clusters to be totally random, but rather to exhibit strong *short-range* correlations due to dipole-dipole interactions. This short-range order was taken into account explicitly by Kirkwood [18], who introduced the so-called Kirkwood factor g: $\langle \mathbf{m}_s \cdot \mathbf{m}_s\rangle = gsd^2$, where $g>1$. Obviously this constant is difficult to calculate for a given material, but luckily it appears in both the numerator and denominator of $\phi(t)$ and consequently Eq. (6) reduces to the expression

$$\phi(t) = \frac{\sum_s n_s s \exp(-t/\tau_s)}{\sum_s n_s s}. \tag{7}$$

If we insert Eq. (7) into Eq. (1) and split the dielectric constant into its real and imaginary parts $\epsilon(\omega)=\text{Re}\epsilon(\omega)+i\text{Im}\epsilon(\omega)$ we find

$$\frac{\text{Re}\epsilon(\omega)-\epsilon_\infty}{(\epsilon_0-\epsilon_\infty)} = \frac{\sum_s n_s s \Big/ [1+(\omega\tau_s)^2]}{\sum_s n_s s},$$

$$\frac{\mathrm{Im}\epsilon(\omega)}{(\epsilon_0-\epsilon_\infty)}=\frac{\sum_s n_s s(\omega\tau_s)\Big/[1+(\omega\tau_s)^2]}{\sum_s n_s s}+\frac{4\pi\sigma_{\mathrm{dc}}/(\epsilon_0-\epsilon_\infty)}{\omega}. \tag{8}$$

Thus we see that we have expressed both the broadband dielectric constant and loss in terms of the cluster size distribution and the cluster lifetimes.

C. Relaxation times τ_s

The rotational relaxation time of the clusters is determined by the free energy barrier that involves breaking the hydrogen bonds with the surrounding liquid. We argue that this is given by an Arrhenius form, where the energy barrier scales with the surface area of the cluster as the cluster attempts to break the cage of mobile liquidlike molecules in which it is confined:

$$\tau_s=\tau_0\exp(\bar{\mu}s^{2/3}/k_BT). \tag{9}$$

Here the attempt time τ_0 is of the order of 10^{-12} s, while the energy for breaking a typical bond $\bar{\mu}\approx\sigma$ can be expected to scale with the surface energy per molecule. We will estimate the numerical values of these parameters below in the context of the theory for glycerol.

While Eq. (9) appears rather innocent and perfectly reasonable, its consequences are manifold, lying at the very basis of our approach. These consequences are explained in the next section.

D. Mesoscale thermodynamic theory for the cluster distribution $n_s(T,p)$

The most interesting part of the theory is the estimate of the cluster size distribution $n_s(T,p)$. In this section we provide a thermodynamic theory to estimate this crucial quantity. Our main assertion is that in the supercooled liquid the state of the system is characterized by the existence of a maximal cluster size $s_{\max}$ which is estimated below from experimental data. To have a quick estimate of the expected value of $s_{\max}$, note that, if the relaxation time as expressed in Eq. (9) were correct, we could estimate the size of the largest clusters as $s_{\max}$ just from looking at the longest relaxation times observed experimentally. We thus write

$$s_{\max}\sim[(k_BT/\bar{\mu})\ln(t_{\max}/\tau_0)]^{3/2}, \tag{10}$$

where $t_{\max}$ is the longest time scale observed in the broadband spectrum. For example, for glycerol $t_{\max}\sim10^4$ s and $\bar{\mu}\sim2k_BT$ [19]; then $s_{\max}\sim100$. We will see below that in order of magnitude this estimate is fully justified by the present theory. Thus, in developing a thermodynamic theory, we need to invoke a constraint on the size of the maximal cluster. In other words, we treat the heterogeneities in glycerol in terms of a mesoscale distribution of clusters with a range of size $s_{\min}<s<s_{\max}$ in a more mobile bath of liquidlike molecules. This approach of applying to the glass-forming liquid statistical mechanics subject to constraints follows up our previous analysis of other glass-forming liquids (cf. [20–22]). Note that this approach is radically different from the proposition of [15,16] where a mysterious "strain energy" term was invoked to explain why larger clusters are not present in the theory.

The intensive numbers of such clusters of size s are $n_s(p,T)=N_s(p,T)/M$, and the probability that an individual glycerol molecule belongs to a cluster of size s is $c_s=n_ss$. We denote below the number of molecules belonging to the clusters and to the liquid phase by M_c and M_ℓ, respectively, with $M_c+M_\ell=M$. To describe the mesoscale thermodynamics we assume that in a cluster at temperature T and pressure p we have an intensive contribution to the chemical potential

$$\mu_c=u_c+pv_c-Ts_c, \tag{11}$$

where the subscript c stands for "cluster" and u_c, v_c, and s_c are, respectively, the internal energy per molecule, the volume per molecule, and the entropy per molecule in the clusters. Similarly, in the liquidlike phase we can write for the intensive contribution to the chemical potential

$$\mu_\ell=u_\ell+pv_\ell-Ts_\ell, \tag{12}$$

where the subscript ℓ stands for liquid and u_ℓ, v_ℓ, and s_ℓ are, respectively, the internal energy per molecule, the volume per molecule, and the entropy per molecule in the mobile liquidlike phase. We expect that $u_c<u_\ell$ because the hydrogen bonds in the clusters are less distorted; $s_c<s_\ell$ because of the greater number of rotational degrees of freedom in the mobile phase; and $v_c<v_\ell$ because of the higher density of more solidlike glycerol compared to the liquid. All these intensive thermodynamic variables are in principle functions of temperature T and pressure p. Apart from these extensive contributions to the Gibbs free energy $M_c\mu_c+M_\ell\mu_\ell$ where $M_c=\Sigma_sN_ss=M\Sigma_sn_ss=M\Sigma_sc_s$, we need to consider two other crucial contributions to the total free energy.

First, there is a surface energy contribution U_{surface} due to the interface between each cluster and its surrounding bath. This scales as the surface area of each cluster and therefore we can write

$$U_{\mathrm{surface}}=\sigma\sum_s N_s s^{2/3}, \tag{13}$$

where σ is the surface energy per molecule. Obviously, the value of σ will turn out to be crucial in determining the distribution of cluster sizes. To estimate its size, note that σ could be as large as a hydrogen bond energy, but in fact we expect it to be smaller because the mobile phase is also partially hydrogen bonded. Thus we expect $\sigma\approx u_\ell-u_c$, which is some fraction of a hydrogen bond energy.

Second, there will be an entropic contribution due to all possible spatial configurations of clusters in the glassy liquid. This is an important contribution to the free energy, favoring small clusters and being responsible for the β peak when it exists. In taking the entropy explicitly into account, we deviate once more from all previous theories; we cannot see why the entropy was not considered before. We can estimate this entropy by sequentially placing all clusters in the available volume starting with the largest [21]. Thus the volume available to the largest clusters is $V=M_cv_c+M_\ell v_\ell$. The volume available to the next largest clusters is $V-s_{\max}N_{s_{\max}}v_c$,

etc. As we proceed in this manner, the entropy of mixing is given by the expression

$$S_{\rm mix} = -k_B \sum_s \mathcal{N}_s [x_s \ln x_s + (1-x_s)\ln(1-x_s)], \quad (14)$$

where k_B is Boltzmann's constant and $\mathcal{N}_s = (V/v_c - \Sigma_{s'>s} N_{s'}(s'))/s$ is the number of boxes available to clusters of size s, while $x_s = N_s/\mathcal{N}_s$ is the fraction that is occupied. Thus

$$x_s = \frac{c_s}{\sum_{s'=s_{\rm min}}^{s} c_{s'} + \Delta}$$

$$\Delta \equiv (v_\ell/v_c)c_\ell, \quad (15)$$

where c_ℓ is the fraction of molecules in the liquidlike phase, and of course the sum of the concentrations of molecules in the condensed and liquidlike phases obeys

$$c_c + c_\ell = 1.0. \quad (16)$$

At this point we introduce v as the average volume per glycerol molecule in our system, where of course

$$v = c_c v_c + c_\ell v_\ell. \quad (17)$$

We can now solve Eqs. (16) and (17) for c_c and c_ℓ in terms of these three volumes per molecule and write the crucial sum rule

$$\sum_{s=s_{\rm min}}^{s_{\rm max}} c_s \equiv c_c = \frac{v - v_\ell}{v_c - v_\ell}. \quad (18)$$

This is the crucial constraint on the thermodynamic theory; we will impose this constraint on our solution by choosing the largest cluster $s = s_{\rm max}$ such that Eq. (18) is obeyed.

The free energy for our system is given by the expression

$$F = U - TS = M_c\mu_c + M_\ell\mu_\ell + \sigma\sum_s N_s s^{2/3} + k_B T \sum_s \mathcal{N}_s [x_s \ln x_s + (1-x_s)\ln(1-x_s)] \quad (19)$$

and the chemical potential of a cluster of size s is given by

$$\mu_s = s\mu = \partial F/\partial N_s = \mu_c s + \sigma s^{2/3} + k_B T\left(\ln x_s + \sum_{s'>s} (s/s')\ln(1-x_{s'})\right). \quad (20)$$

Rewriting Eq. (20) for the chemical potential per molecule in the cluster,

$$\mu = \mu_c + \sigma s^{-1/3} + k_B T\left((1/s)\ln x_s + \sum_{s'>s} (1/s')\ln(1-x_{s'})\right). \quad (21)$$

The chemical potential in the liquid phase must be the same as that calculated for the clusters and given by Eq. (21), and therefore

$$\mu = \mu_\ell + k_B T(v_\ell/v_c)\sum_s (1/s)\ln(1-x_s). \quad (22)$$

We can use Eq. (22) to define a new chemical potential $\mu' = \mu - (\mu - \mu_\ell)/(v_\ell/v_c) - \mu_c$ which together with Eq. (21) then obeys

$$\mu' = \sigma s^{-1/3} + k_B T\left((1/s)\ln[x_s/(1.0-x_s)] - \sum_{s'<s} (1/s')\ln(1-x_{s'})\right). \quad (23)$$

In this form it is easy to solve these equations numerically in a sequential fashion, starting with $s = s_{\rm min}$. Using Eq. (23) we see that the concentration of the smallest clusters $c_{s_{\rm min}}$ obeys

$$\mu' = \sigma s_{\rm min}^{-1/3} + k_B T(1/s_{\rm min})\ln(c_{s_{\rm min}}/\Delta). \quad (24)$$

To estimate $s_{\rm min}$ we note that in three dimensions a "cluster" must have at least 2–3 molecules in each direction to be identifiable as a cluster. Thus the minimal value of s is about 20. We do not know μ' *a-priori,* depending as it does on the details of the energies, structure, and entropies in the clusters and liquidlike phases, so instead we have taken the data from [23] for the average size of the clusters $s_{\rm av} = \Sigma_s s c_s/\Sigma_s c s$. From this we determined the value of $c_{s_{\rm min}}$; for example we find a value at $T = 200$ K which is $c_{s_{\rm min}} = c(s=20) = 0.0035$ and determined everything else from that. We are now in a position to estimate μ' from Eq. (24). Then all the values of c_s for $s > s_{\rm min}$ follow from Eqs. (23) in order until Eq. (18) is satisfied. We will see below that for glycerol the largest s predicted by the theory is about 100. The reader should note that we are not making any effort here to best fit the data of glycerol; rather we are after the essential qualitative issues. It is surprising in fact that we get semiquantitative agreement below. Needless to say, one can fit everything much more closely to experiment, but this is not the main aim of this paper.

III. PREDICTIONS FOR BROADBAND DIELECTRIC SPECTROSCOPY: THE CASE OF GLYCEROL

Examining our expressions for the distribution of clusters given by Eqs. (23) and (24), we note that, in order to apply the theory to a particular substance, we are missing the value of the surface energy σ, say for glycerol. Since this quantity appears inside exponential forms we need a rather accurate value for comparison with experimental data. One approach would be to fit our dielectric spectra at one temperature and then use the fitted parameters to predict its form at different temperatures. Here we have taken a slightly different approach, using available glycerol data. There are two types of data. The first concerns the average volumes per glycerol molecule in the liquid, solid, and glassy phases. For v_ℓ we employed data of liquid glycerol at room temperature, giving $v_\ell = 121$ Å^3. For v_c and v we took data from [24], which give for the cluster phase $v_c = 110$ Å^3 and for the glassy phase $v = 113$ Å^3 at atmospheric pressure. These numbers were used to estimate the constraint given by Eq. (18). The second type of data we have at our disposal concerns the size

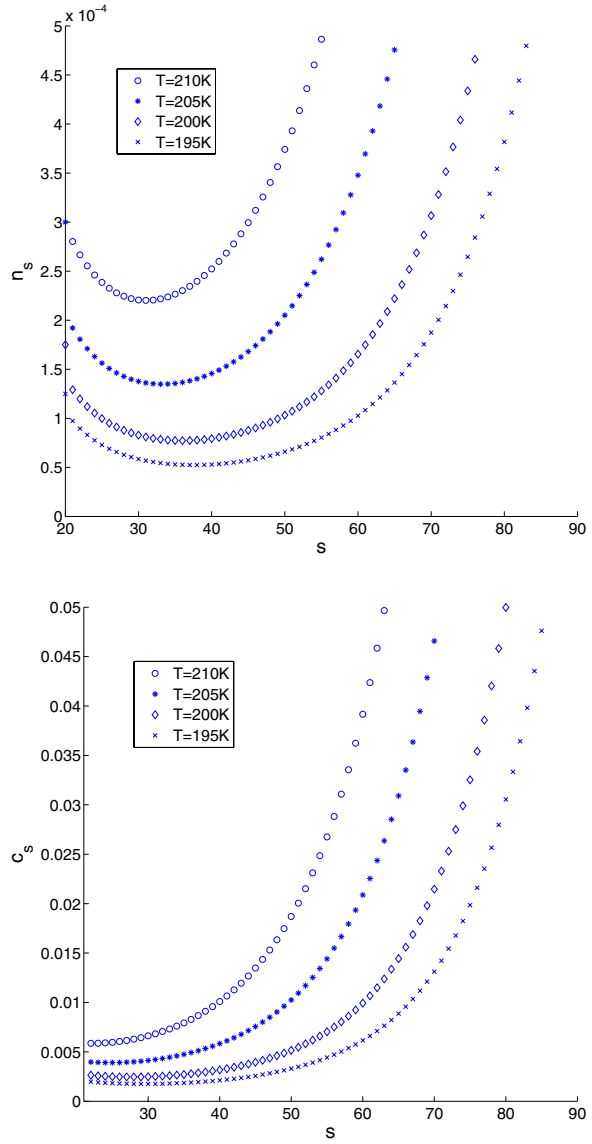

FIG. 3. (Color online) Upper panel: Cluster size distribution n_s versus s for temperatures $T=210$, 205, 200, and 195 K. Lower panel: Concentration of molecules c_s as a function of cluster size s for the same temperatures.

of dynamic heterogeneities as a function of temperature. We have taken data from [24] for the average size of such heterogeneities $s_{\mathrm{av}}=\Sigma_s s c_s/\Sigma_s c_s$. The data used were $s_{\mathrm{av}}(T=210\ \mathrm{K})\approx 50$, $s_{\mathrm{av}}(T=205\ \mathrm{K})\approx 58$, $s_{\mathrm{av}}(T=200\ \mathrm{K})\approx 67$, and $s_{\mathrm{av}}(T=195\ \mathrm{K})\approx 73$. These two pieces of information can be accommodated in our theory using $\sigma/k_B=320$ K or $\sigma/k_BT\approx 1.6$. We then predict the maximal cluster sizes at these temperatures to be $s_{\max}(T=210\ \mathrm{K})\approx 63$, $s_{\max}(T=205\ \mathrm{K})\approx 72$, $s_{\max}(T=200\ \mathrm{K})\approx 81$, and $s_{\max}(T=195\ \mathrm{K})\approx 87$. Using these data we then studied the theoretical predictions for glycerol.

As noted above, the distribution of clusters between $s_{\min}$ and $s_{\max}$ is strongly dependent on surface energy. Using $\sigma/k_B=320$ K, we plot the cluster size distribution n_s and the density of molecules as a function of cluster size s for dry glycerol at $T=210$, 205, 200, and 195 K. Small clusters are favored at higher temperatures, when the entropy of mixing

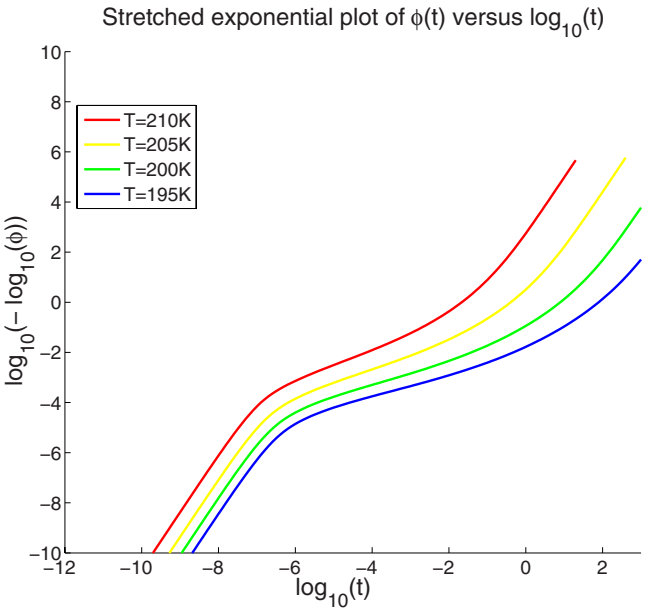

FIG. 4. (Color online) Stretched exponential plot of $\phi(t)$ showing an approximate straight line over about six orders of magnitude in time for temperatures $T=210$ (leftmost), 205, 200, and 195 K (rightmost).

dominates the distribution (see Fig. 3). But as the temperature is reduced, larger clusters are favored, as energy dominates the distribution. In general, the distribution is bimodal, favoring small and large clusters at the expense of intermediate sizes (see Fig. 3). We note that the sharp cut of the distribution at $s=s_{\max}$ is a bit artificial; in reality, one can expect a sharply decaying tail at s values slightly larger than $s_{\max}$. We do not expect such minor details to influence the main results presented below.

We are now in a position to calculate both $\phi(t)$ from Eq. (7) and the real and imaginary parts of the dielectric function from Eq. (8). This quantity had been fitted phenomenologically to a stretched exponential form, $\phi(t)\sim\exp-(t/\tau)^{\beta_K}$, a form referred to in the literature as the Kohlrausch-Williams-Watts relaxation function (see, for example, [25]). To see whether this form is justified by the present theory we plot our computed function in the appropriate coordinates (see Fig. 4). Indeed, a stretched exponential with $0.4<\beta_K<0.66$ gives an acceptable fit over a broad range of time scales $t_{\min}\sim 10^{-6}\ll t\ll t_{\max}\sim 10^{0}$ s, with deviations at both shorter and longer times. We note that β_K is temperature dependent and stress that the stretched exponential form has a limited value in the sense that it is just an acceptable fit in a limited range for a very different function. Nevertheless, the numerical value of β_K and its variability with the experimental conditions are both confirmed by experiments in glycerol; see, for example, [8,25].

Of greater interest is the dielectric spectrum and loss function (see Fig. 5) which correspond to the distributions shown in Fig. 3 with $T=210$, 205, 200, and 195 K, respectively. The real part of the dielectric constant $\mathrm{Re}\epsilon(\omega)$ starts to decline from ϵ_0 to its asymptotic value of ϵ_∞ at around $\omega\approx\omega_{\max}$ but takes several frequency decades to achieve as-

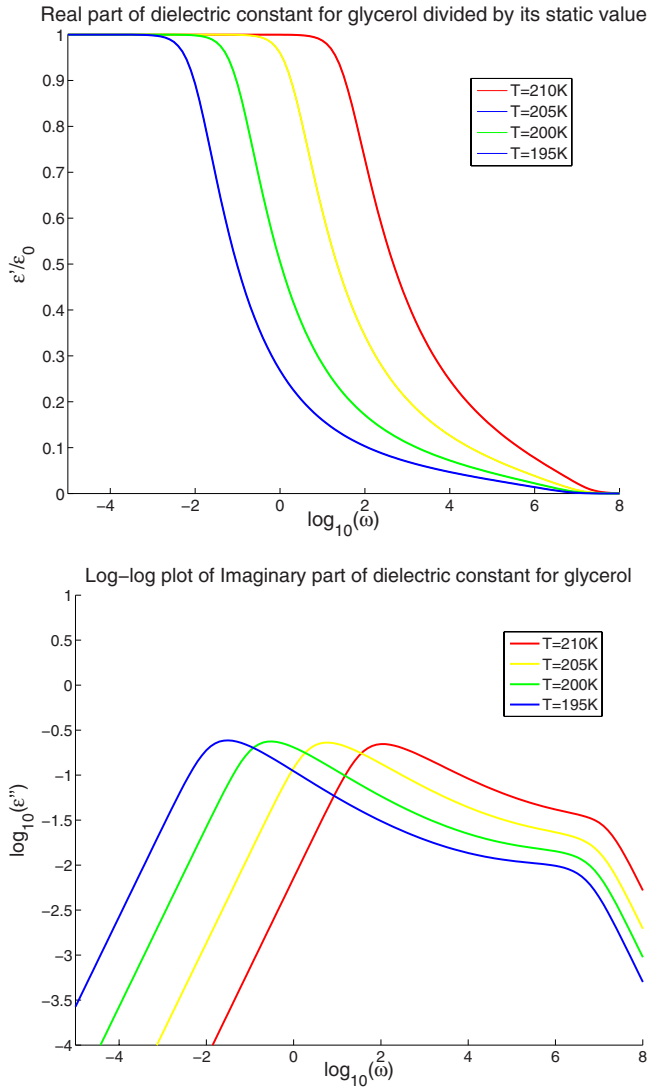

FIG. 5. (Color online) Upper panel: Real part of the dielectric spectrum $\epsilon'(\omega)/\epsilon_0$ versus $\log_{10}(\omega)$ for temperatures $T=210$, 205, 200, and 195 K. Lower panel: A log-log plot of the dielectric loss $\log_{10}[\epsilon''(\omega)]$ versus $\log_{10}(\omega)$ for temperatures $T=210$ (rightmost), 205, 200, and 195 K (leftmost).

ymptotia. We refer the reader to [8,25] and references therein to note that both the qualitative form of $\mathrm{Re}\epsilon(\omega)$ and its quantitative details are in close correspondence with experiments in glycerol (as well as in glycerol-rich water mixtures).

The shape of $\mathrm{Im}\epsilon(\omega)$ is controlled by the shape of the cluster size distribution. There is always a clear α peak at low frequencies $\omega_{\max}$ defined by $d\,\mathrm{Im}\epsilon(\omega_{\max})/d\omega_{\max}=0$, associated with the largest clusters. Very roughly $\omega_{\max} \sim 1/t_{\max}$. But we can also see at all temperatures a clear excess wing at higher frequencies. As the temperature is lowered the excess wing becomes slightly less pronounced. Note that the very sharp fall-off at the highest frequency is due to our neglect of the liquid phase fast-relaxing contribution. For a full quantitative comparison between theory and experiment, this contribution should be taken into account; this will be done in a future presentation.

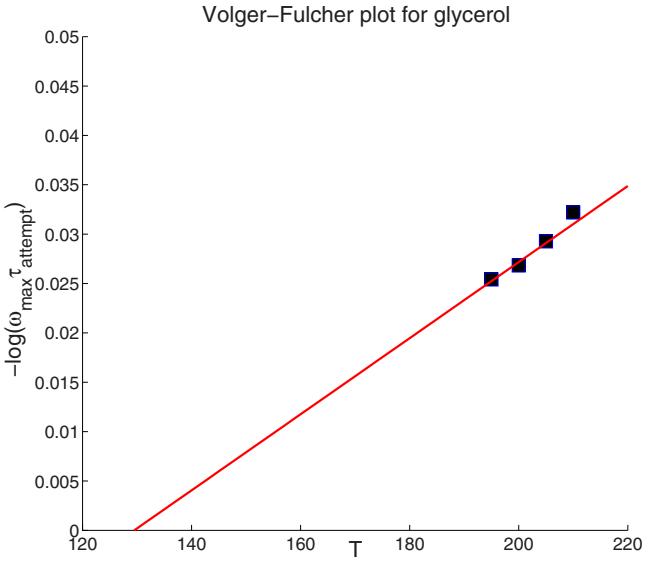

FIG. 6. (Color online) $\omega_{\max}$ for the dielectric loss for temperatures $T=210$, 205, 200, and 195 K plotted in a Vogel-Fulcher form. The plot underlines the irrelevance of T_v as a physical parameter, since it is so far removed from the region of linear fit. The theory presented here actually does not predict a true divergence of the relaxation time; it only becomes superexponentially large.

The next interesting question is whether we can justify theoretically the Vogel-Fulcher plots. To answer this question we plot the computed values of $\omega_{\max}$ in a Vogel-Fulcher form as in Eq. (3) (see Fig. 6). In this plot we display, on purpose, the whole temperature range including T_v to stress the absurdity of such a fit. Nevertheless, a straight line can be fitted through the computed points. Using the same (unphysical) attempt time of $\ln \tau_v=-35.9$ as in the experimental fits for glycerol, the straight line best fit gives $T_v=129$ K and a fragility $D=20.0$. This should be compared with $T_v=125$ K and $D=22.7$, which are the numbers reported experimentally. Our conclusion is that the theory explains both the stretched exponential fits to the relaxation function and the Vogel-Fulcher fit, but both are fundamentally meaningless, and should be replaced by a theory of the type proposed here.

IV. THE ROLE OF SURFACE ENERGY: CLUSTER DISTRIBUTIONS AND DIELECTRIC SPECTRA

To understand the experimental results for glycerol, we chose the crucial parameter σ from structural data. In this section we ask a different question—what is the qualitative influence of the surface energy σ on cluster size distributions and dielectric responses? In particular, we are interested in the possibility of generating a distinct β peak by changing only one molecular parameter, which is σ. To study this question we fix $s_{\max}=100$ and $T=200$ K and study the effect of changing the surface energy. We choose four values $\sigma/k_BT=1.0$, 1.25, 1.5, and 1.75. As we increase σ, the average cluster size increases: $s_{\mathrm{av}}(\sigma/k_BT=1.0)\approx 48$, $s_{\mathrm{av}}(\sigma/k_BT=1.25)\approx 76$, $s_{\mathrm{av}}(\sigma/k_BT=1.5)\approx 87$, and $s_{\mathrm{av}}(\sigma/k_BT=1.75)\approx 91$. The complete distribution can be seen in Fig. 7. As σ

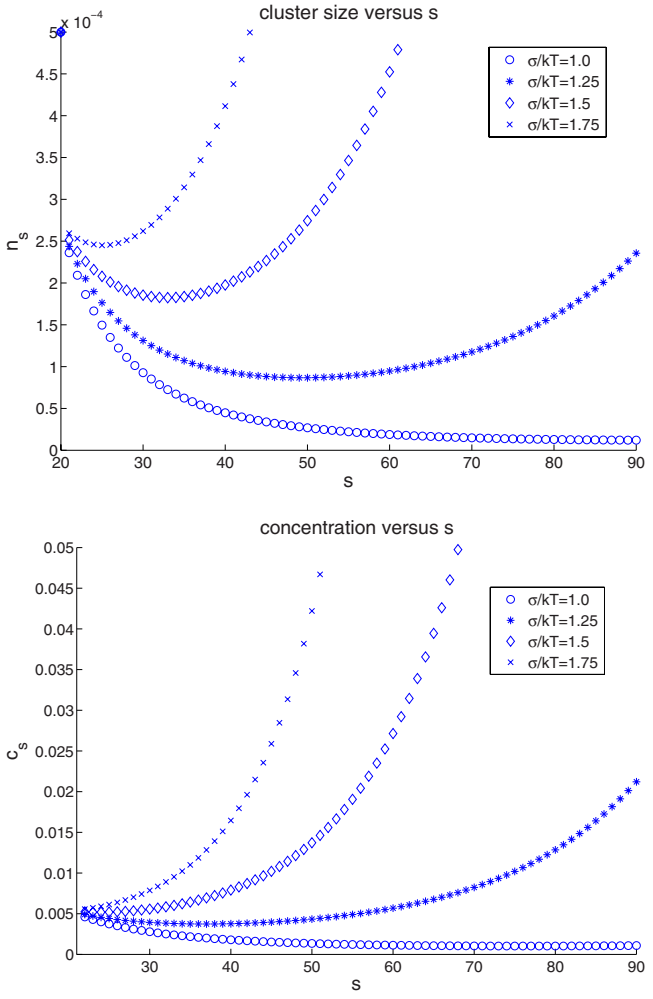

FIG. 7. (Color online) Upper panel: Cluster size distribution n_s versus s for $\sigma/k_BT=1.0$, 1.25, 1.5, and 1.75. Lower panel: Concentration of molecules c_s as a function of cluster size s for temperatures $\sigma/k_BT=1.0$, 1.25, 1.5, and 1.75.

increases, large clusters are favored over small clusters; σ has a crucial qualitative influence on the bimodality of the distribution.

The change in surface energy must also influence the dynamics. We asserted that the rotational lifetimes τ_s of clusters of size s are given by Arrhenius forms where the energy barrier scales with the surface area of the cluster, as the cluster attempts to break the cage of mobile liquidlike molecules in which it is confined. The energy for breaking a typical bond can be expected to scale with the surface energy σ. In Fig. 8 we have plotted the behavior of $\phi(t)$ in a stretched exponential form to show scaling in time for $\sigma/k_BT=1.0$, 1.25, 1.5, and 1.75. Note that as σ increases the stretched exponential regime increases due to a more pronounced α peak, while at low surface energies the high-frequency β peak destroys this kind of scaling.

Of greater interest are the dielectric spectra and loss functions (see Fig. 9) which correspond to the distributions shown in Fig. 7 with $\sigma/k_BT=1.0$, 1.25, 1.5, and 1.75, respectively. The shape of $\mathrm{Re}\epsilon(\omega)$ corresponds to a decline from ϵ_0 to ϵ_∞ starting at $\omega_{\max}$, but one interesting point is that the β

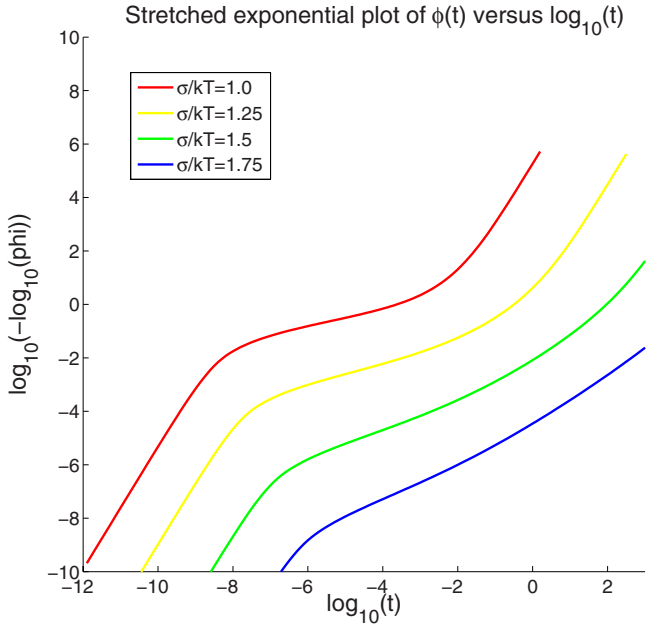

FIG. 8. (Color online) Stretched exponential plot of $\phi(t)$ to show scaling regime in time for $\sigma/k_BT=1.0$, 1.25, 1.5, and 1.75.

peak can lead to a shoulder here also. The shape of $\mathrm{Im}\epsilon(\omega)$ is again controlled by the cluster size distribution. There is always a clear α peak at low frequencies. But for lower values of the surface energy, small clusters are encouraged, resulting in a prominent β peak at high frequencies. As the surface energy increases the β peak becomes less pronounced turning first into a shoulder at intermediate frequencies (see Fig. 9), and finally into the anomalous scaling observed in many experimental data sets (see Fig. 9). These interesting qualitative findings will be turned into quantitative comparisons with experiments in different materials in a later presentation.

V. BDS IN CONFINED GEOMETRIES

In this section we discuss the BDS of glycerol in confined geometries. We refer here in particular to the experimental studies reported in [26], in which it was shown that glycerol could be confined in pores whose diameter d can be as small as $d=2.5$ nm in size without seeing any appreciable effect in the position of the α maximum or its amplitude. Since we expect that the maximum size cluster should be limited by the size of pores, it appears surprising that there is no confinement effect in the spectra. If our arguments are correct as presented in this paper, there must be a point at which the dielectric loss will be strongly affected by confinement. To estimate where this should happen we equate the volume of the pore to the volume of the largest cluster, i.e.,

$$\pi d^3/6 \approx s_{\max} v_c. \tag{25}$$

Using our estimates of v_c and referring to the temperatures employed in [26], we find that confinement effects are expected to appear when the diameter satisfies $d \leq 2.5$ nm. Thus the experiment just missed the confinement effect by a

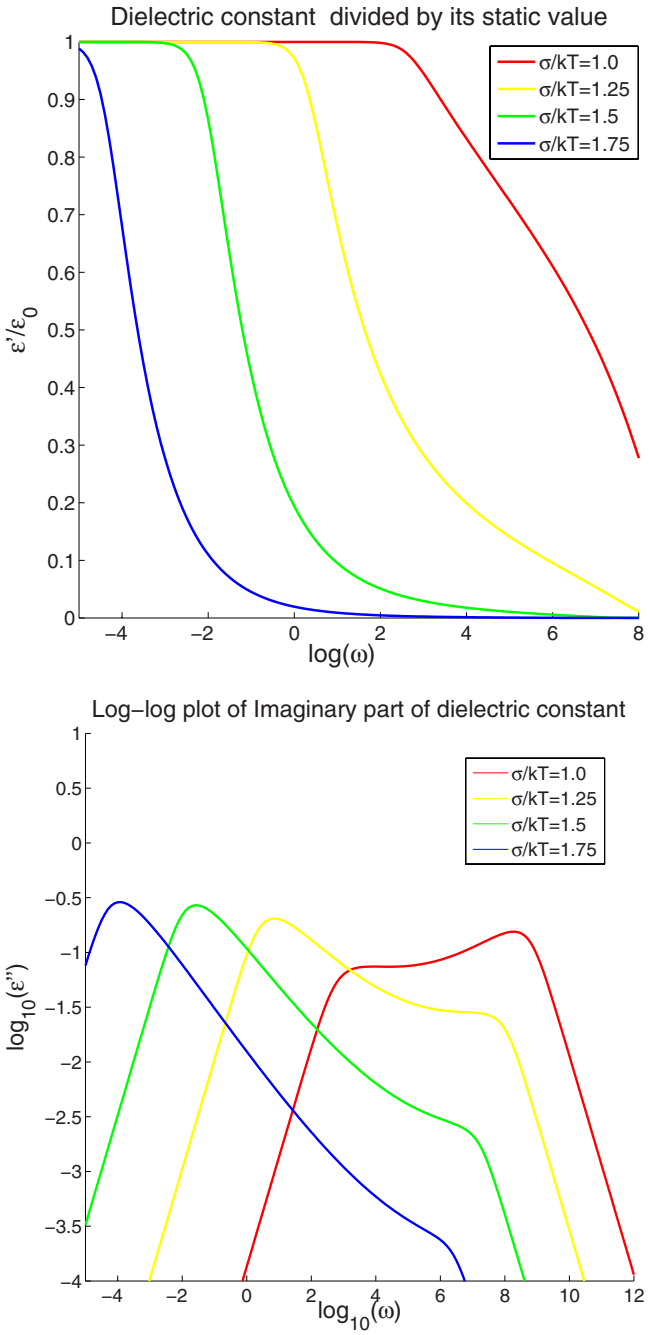

FIG. 9. (Color online) Upper panel: Real part of the dielectric spectrum $\epsilon'(\omega)/\epsilon_0$ versus $\log_{10}(\omega)$ for $\sigma/k_BT=1.0$ (rightmost), 1.25, 1.5, and 1.75 (leftmost). Lower panel: A log-log plot of the dielectric loss $\log_{10}[\epsilon''(\omega)]$ versus $\log_{10}(\omega)$ for the same values of σ/k_BT as in the upper panel.

hair. In Fig. 10 we present our own prediction as to how the expected position of $\omega_{\max}$ depends on the confining pore diameter. Note that there is no effect down to a critical pore diameter, below which the shift in $\omega_{\max}$ is dramatic. Here we are plotting the shift as a function of pore diameter at fixed temperature. We also note that, as a function of temperature, clusters tend to grow or shrink, and therefore confinement effects should be more dramatic at lower temperatures where the unconfined clusters are expected to be larger.

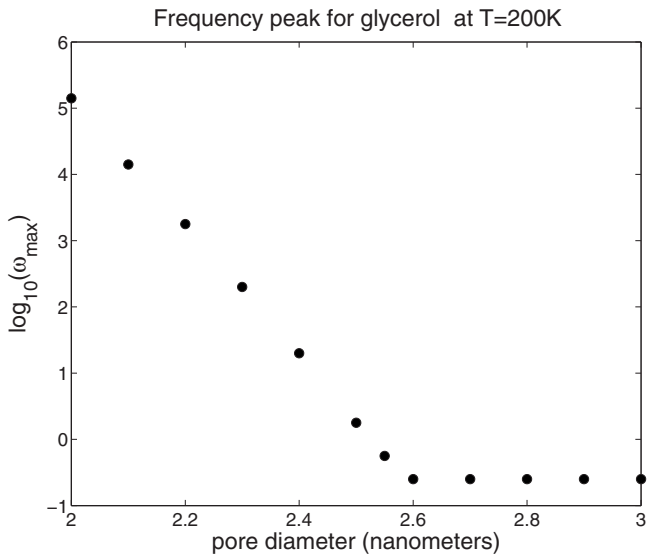

FIG. 10. Shift in expected position of $\omega_{\max}$ as a function of confining pore diameter. Note that no effect appears until a critical pore diameter, after which the shift is dramatic.

VI. THE dc CONDUCTIVITY AND THE DATA COLLAPSE

One particularly interesting aspect of the glycerol measurements, i.e., the data collapse shown in Fig. 2, was not used yet to challenge the theory. Note that the experimental data collapse includes the clearly identified dc branch below frequencies $\omega/\omega_{\max}\approx 10^{-3}$. In this section we explain why the dc conductivity scales together with the peak $\omega_{\max}$ of the α peaks and then demonstrate the data collapse of the theoretical spectra.

Consider a charge carrier (say a proton) under a dc voltage drop. It is natural to assume that this charge carrier can very rapidly move on a cluster of size s, but it is practically jammed when in the liquidlike phase. Thus it can swiftly move a distance of the cluster size $R_s\sim s^{1/3}a$, where a is the inner length scale of the order of $v_c^{1/3}$. After such motion the charge carrier becomes jammed again until a time of the order of τ_s, after which the charge carrier can encounter a new cluster of a different size s'. Note that here we assume that the rotational relaxation time and the lifetime of the cluster are of the same order of magnitude. Another way of stating the dynamics just described is in terms of a local diffusion constant

$$D_s \sim R_s^2/\tau_s \sim (a^2/\tau_0)s^{2/3}\exp(-\sigma s^{2/3}/k_BT). \qquad (26)$$

Over long periods of time the diffusing particle will be jammed by a series of clusters α. The resultant average particle diffusion $D(T)$ can then be estimated as follows. In a long time $t=\Sigma_\alpha t_\alpha$, the associated mean square displacement obeys $R(t)^2=\Sigma_\alpha R_\alpha^2$. Thus the time-averaged diffusion constant is $D(T)=\lim_{t\to\infty} R(t)^2/t$, while replacing the time average by an ensemble average over the cluster distribution results in the expression

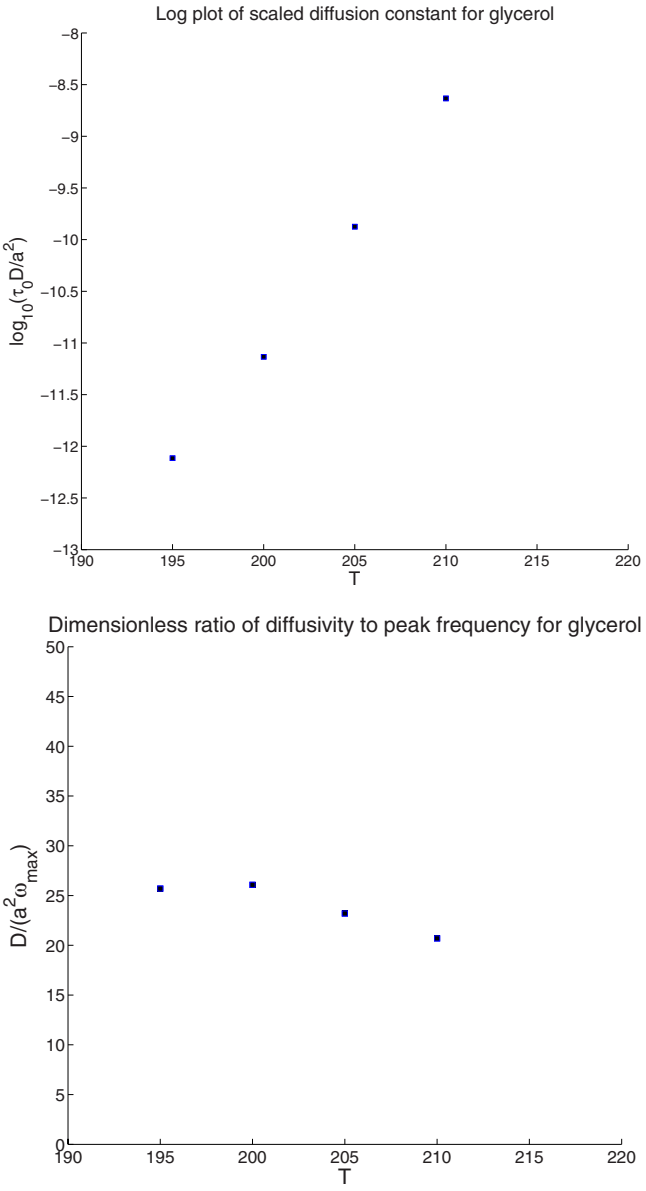

FIG. 11. (Color online) Upper panel: Log plot of average diffusion constant $D(T)$ for glycerol at temperatures $T=210$, 205, 200, and 195 K. Lower panel: The diffusion constant divided by the peak frequency of the α peak $D(T)/\omega_{\max}(T)$ for the same temperatures.

$$D(T) = (a^2/\tau_0)\frac{\sum_s n_s s^{2/3}}{\sum_s n_s \exp(\sigma s^{2/3}/k_B T)}. \tag{27}$$

Let us plot Eq. (27) using the parameters we used for glycerol previously. In the upper panel of Fig. 11, we have plotted the logarithm of $D(T)$ for $T=210$, 205, 200, and 195 K. The diffusion coefficient changes by about four orders of magnitude in the given range of temperatures. Nevertheless, to a very good approximation,

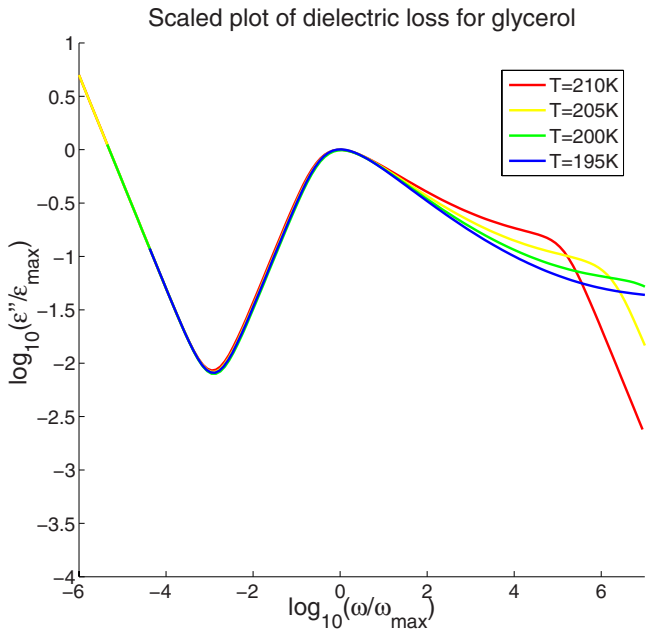

FIG. 12. (Color online) Data collapse with the theoretical spectra: a rescaled version of the plots in Fig. 5 to which the dc conductivity contribution to the loss has been added.

$$D(T) \sim a^2 \omega_{\max}(T). \tag{28}$$

This is demonstrated in the lower panel, where despite the large variation in the diffusion coefficient it scales as the peak of the α spectrum $\omega_{\max}(T)$.

At this point we recall the Einstein relation between the dc conductivity $\sigma_{\rm dc}$ and the diffusion coefficient of the charge carriers:

$$\sigma_{\rm dc} = \frac{nq^2 D(T)}{k_B T}, \tag{29}$$

where n is the density of charge carriers, which for hydrogen-bonded liquids we assume to be the density of free protons, and $q=+e$ is their charge. Equation (29) implies that

$$\sigma_{\rm dc} \sim \frac{a^2 n q^2}{k_B T}\omega_{\max}(T). \tag{30}$$

Accordingly, we conclude that the whole BDS spectrum should remain invariant to a rescaling of the frequency by $\omega_{\max}(T)$, for a reasonable range of T, as was indeed done with the experimental spectra. We present our theoretical spectra in a similar manner, rescaling the frequency ω and the amplitude $\epsilon''(\omega)$ by the frequency and amplitude of the α peak. The result of the exercise is shown in Fig. 12, without any attempt to refit any of the material parameters. Note the data collapse, with the excess wings failing to collapse perfectly. In fact, one could get an excellent collapse here by changing the exponent in the relaxation rate from $s^{2/3}$ to $s^{0.57}$. Whether this indicates that the clusters are not compact but have a fractal structure is not known at this moment in time. We found no justification for such refits at this point, since the neglected fast-relaxing contribution due to the liquid phase is also needed here for a quantitative comparison. As

we said above, we defer the detailed quantitative fits to a future presentation where theory and experiments will be compared in full detail.

VII. DISCUSSION

We have shown how a relatively simple model of uncorrelated cluster relaxations can account, without much parameter fitting, for the qualitative and even the quantitative aspects of the observed BDS in hydrogen-bonded liquids. The theory was demonstrated for glycerol, but obviously with a mere change of molecular parameters it should apply to a broad range of other hydrogen-bonded liquids. It was demonstrated explicitly that the α and β regions of the dielectric spectra can in principle stem from the very same physics, and their relative amplitudes are determined by the relative population of small or large clusters. The relative population is determined by entropic effects, which were explicitly taken into account in our thermodynamic theory, and by the surface energy per molecule in addition to the temperature. Applications to other materials will be presented elsewhere.

ACKNOWLEDGMENTS

This work was supported in part by the German-Israeli Foundation and the Minerva Foundation, Munich, Germany. The authors are grateful to Yuri Feldman and Alexander Puzenko for introducing them to the subject and for sharing with them their knowledge and experimental results.

[1] D. W. Davidson and R. H. Cole, J. Chem. Phys. **19**, 1484 (1951).
[2] G. P. Johari and E. Whalley, Faraday Symp. Chem. Soc. **6**, 23 (1972).
[3] C. A. Angell, J. Non-Cryst. Solids **13**, 131 (1991).
[4] K. L. Ngai, R. W. Rendell, and D. J. Plazek, J. Chem. Phys. **94**, 3018 (1991).
[5] P. Lunkenheimer, A. Pimenov, M. Dressel, Yu. G. Goncharov, R. Böhmer, and A. Loidl, Phys. Rev. Lett. **77**, 318 (1996).
[6] U. Schneider, R. Brand, P. Lunkenheimer, and A. Loidl, Phys. Rev. Lett. **84**, 5560 (2000).
[7] K. L. Ngai, J. Non-Cryst. Solids **275**, 7 (2000).
[8] A. Puzenko, Y. Hayashi, Y. E. Ryabov, I. Balin, Y. Feldman, U. Kaatze, and R. Behrends, J. Phys. Chem. B **109**, 6031 (2005).
[9] W. Gotze and L. Sjogren, Rep. Prog. Phys. **55**, 241 (1992).
[10] R. Behrends, K. Fuchs, U. Kaatze, Y. Hayashi, and Y. Feldman, J. Chem. Phys. **124**, 144512 (2006).
[11] D. W. Davidson and R. H. Cole, J. Chem. Phys. **18**, 1417 (1950).
[12] R. Zondervan, F. Kulzer, G. C. G. Berkhout, and M. Orrit, Proc. Natl. Acad. Sci. U.S.A. **104**, 12628 (2007).
[13] A. Geiger and H. E. Stanley, Phys. Rev. Lett. **49**, 1749 (1982).
[14] R. V. Chamberlin, Phys. Rev. B **48**, 15638 (1993).
[15] D. Kivelson and G. Tarjus, Philos. Mag. B **77**, 245 (1998).
[16] G. Tarjus, D. Kivelson, and P. Viot, J. Phys.: Condens. Matter **12**, 6497 (2000).
[17] J. S. Langer, Phys. Rev. Lett. **97**, 115704 (2006); Phys. Rev. E **73**, 041504 (2006).
[18] J. G. Kirkwood, J. Chem. Phys. **7**, 911 (1939).
[19] This estimate of $\bar{\mu}$ is justified in Sec. III.
[20] E. Aharonov, E. Bouchbinder, H. G. E. Hentschel, V. Ilyin, N. Makedonska, I. Procaccia, and N. Schupper, Europhys. Lett. **77**, 56002 (2007).
[21] H. G. E. Hentschel, V. Ilyin, N. Makedonska, I. Procaccia, and N. Schupper, Phys. Rev. E **75**, 050404(R) (2007).
[22] V. Ilyin, E. Lerner, T.-S. Lo, and I. Procaccia, Phys. Rev. Lett. **99**, 135702 (2007).
[23] L. J. Root and F. H. Stillinger, J. Chem. Phys. **90**, 1200 (1989).
[24] F. Ladieu, C. Thibierge, and D. L'Hôte, J. Phys.: Condens. Matter **19**, 205138 (2007).
[25] Y. Hayashi, A. Puzenko, and Y. Feldman, J. Non-Cryst. Solids **352**, 4696 (2006).
[26] M. Arndt, R. Stannarius, W. Gorbatschow, and F. Kremer, Phys. Rev. E **54**, 5377 (1996).